COMPARISON OF AXISYMMETRIC COMPRESSION TO FLAT ROLLING OF 5083 AND 6082 ALUMINUM ALLOYS

A.Airod[1], R. Petrov[1], R. Colás[2] and Y. Houbaert[1]

[1] Department of Metallurgy and Materials Science, Ghent University,
Technologiepark 903, 9052 Gent, Belgium.
[2] Facultad de Ingeniería Mecánica y Eléctrica, Universidad Autónoma de Nuevo León,
A.P. 149-F, 66451 San Nicolás de los Garza, N.L., Mexico

Keywords: Axisymmetric compression, flat rolling, mean flow stress, texture, aluminium alloys

Abstract

Determination of microstructure-process-properties relationships has relied in recent years on extensive use of laboratory testing, detailed metallographic analysis, as this information can help to develop physically based models. Simulation of industrial hot rolling remains one of the challenges taken-up by metallurgists to obtain the microstructure, including crystallographic texture, encountered in the commercial processes. The objective of this work was to see how well axisymmetric compression could simulate rolling process. In this context, hot uniaxial compression tests and hot flat laboratory rolling of AlMg4.5Mn (AA5083) and AlMgSi1 (AA6082) aluminium alloys were performed at three different temperatures; room temperature, 300 and 400°C, and constant strain rate of 10 s^{-1}. The mean flow stresses in both deformation modes were compared to each other. The experimental data were fitted to the exponential equation proposed by Voce and combined with the hyperbolic-sine relationship to determine the activation energy for both deformation techniques. Special interest was taken in comparing the texture of the materials being processed.

Introduction

Rolling is a mechanical process involved in many metals processing operations, and its simulation remains the main goal of many laboratory-testing techniques. The principal aim of this paper is to see if axisymmetric compression can be a favorable technique to simulate flat rolling. The results obtained from both deformation modes on two different and promoting alloys in the aluminium industry, AA5083 and AA6082, were compared to each other. Whereas the first alloy is widely used in building and for electromechanical components, the second showed its efficiency in the automotive and shipbuilding industry as a concurrent of steel. It is expected that recovery, recrystallization and the orientation of the new grains formed after plastic deformation will be different in the heat treatable AA6082 than in the solid solution hardened AA5083.

The high stalking fault energy of aluminium promotes dynamic recovery, and flow curves saturate at elevated temperatures due to the equilibrium between strain hardening and softening. The suitable constitutive equation that describes this behaviour and provides a good prediction of strength at high strain levels is the one proposed by Voce [1]:

$$\sigma = \sigma_s - (\sigma_s - \sigma_o)\exp(-c\varepsilon) \qquad (1)$$

Where σ_s is the saturation stress, σ_o is the yield stress and C is an empirical parameter.

The mean flow stress (MFS) calculated using rolling data were compared to the MFS derived from the compression tests. These two parameters will be used to calculate the activation

energy (Q_{HW}) responsible for hot working in flat rolling and axisymmetric compression. Comparison of textures will give an idea about the influence of the deformation mode and the working temperature on the orientation of the new grains.

Experimental Procedures

Two different commercial aluminium alloys, AA5083 and AA6082 were tested in axisymmetric compression (ASC) and laboratory flat rolling conditions, Table 1. Samples for axisymmetric compression were machined from plates into cylinders of 15 mm high and 10 mm diameter with their axes normal to the rolling and transversal directions. These tests were conducted in a servo-hydraulic testing machine described elsewhere [2], and were carried out at room temperature (RT), 300 and 400°C at a strain rate of a 10 s^{-1} up to a true strain of 0.5. The samples were cooled in water after testing. The temperature was controlled by inserting a thermocouple into the samples, which were heated 10°C to 20°C above the temperature of interest, kept between two steel plates and brought as fast as possible under the tools in order to minimize the heat losses during the transfer from the furnace to the machine. The load displacement data for the ASC were converted into stress-strain curves after being corrected for origin and machine stiffness assuming constancy of volume and a constant friction coefficient at the specimen-tooling interface.

Table1: Chemical composition, wt.%, of the alloys

	% Cu	% Fe	% Mn	% Mg	% Si	% Al
AlMg4.5Mn	0,15	0,26	0,48	4,03	0,21	Balanced
AlMgSi1	0,058	0,37	0,80	0,90	1,03	Balanced

The rolling tests were made on samples cut from the same plates as for compression, with 15 mm thickness, 65 mm width and 120 mm length. The rolling equipment was a laboratory Carl Wezel Rolling Mill with 320 mm diameter rolls. The sheets were reduced to 50% in 7 passes at RT and in one pass at high temperature.

The microstructure and texture of the samples after ASC and hot rolling were studied qualitatively and quantitatively by means of orientation image microscopy (OIM). The OIM attachment was installed on a Philips XL30 ESEM microscope with a LaB_6 filament. The specimens for OIM were prepared according to the classical procedure (mechanical grinding and polishing up to a 1 μm diamond paste) followed by electrolytic polishing by A2 Struers® agent during 15 seconds at a temperature of 25°C and voltage of 40 volts. The OIM scans of rolled plates were collected in a section perpendicular to the transverse direction (TD), whereas the scans of the axisymetric compressed samples were carried out in a plane perpendicular to the base of the cylinder. The electron backscattering diffraction (EBSD) patterns were acquired and analyzed by means of the TSL® software.

Results and Discussion

Mechanical Working

The flow stresses of both alloys at different temperatures, Figs. 1 and 2, show that AA6082 has a higher strength at room temperature, but this resistance falls at 300°C and 400°C where saturation is reached at early straining. The influence of deformation temperature is less important in the case of AA5083. It can be appreciated in Figs. 1 and 2 that the fit of the

experimental data by Eq. (1) is quite good for both alloys at the different deformation temperatures.
The integration of the areas under the fitted curves allow calculation of the mean flow stress (MFS) in compression according to the following formula:

$$\sigma_{MFS} = \frac{1}{\varepsilon_f - \varepsilon_o} . \int_{\varepsilon_o}^{\varepsilon_f} \sigma . d\varepsilon \qquad (2)$$

Where ε_o and ε_f are the initial and the final true strains.

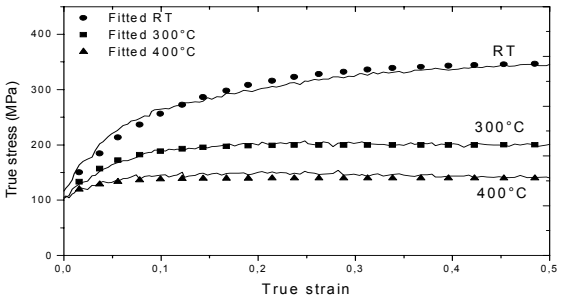

Figure 1: The Flow Stresses of AA 5083 at Different Temperature and έ = $10s^{-1}$ fitted by eq. 1

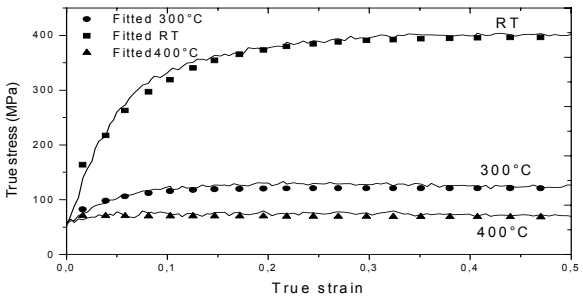

Figure 2: The Flow Stresses of AA 6082 at different Temperature and έ = $10s^{-1}$ fitted by eq.1

The MFS for the rolling process is calculated using the approach proposed by Sims [3] and developed by Maccagno and Jonas [4]:

$$\sigma_{MFS} = \frac{P}{(2/\sqrt{3}).w(R(H-h))^{1/2}.Q} \qquad (3)$$

Where P is the rolling load, w is the width of the sheet, R is the radius of the rolling mills, H and h are the initial and the final thickness, respectively, and Q is a geometrical term.

As pointed out by Tegart and co-workers [5, 6], the steady-state flow stress may be correlated with temperature and strain rate, both under creep and hot working conditions of many different materials, and can be expressed by the more general hyperbolic-sine relationship which covers the whole range of stresses:

$$A(\sinh \alpha\sigma_{MFS})^n = \dot{\varepsilon} \exp(Q_{HW} / RT) \qquad (4)$$

Where έ is the strain rate, R is the universal gas constant, A, α and n are materials constants.

The values of the MFS are used to determine the activation energy of hot axisymmetric compression and hot rolling using the material constants calculated by Airod et al. [7]. AA6082 presents the highest values of the MFS at RT in both deformation modes, Table 2, but at higher temperatures, these values fall by a factor of 3 and 5 respectively, for 300 400°C in compression tests. Such a large drop is not observed in the AA5083, which maintains moderate strength during deformation at high temperature. Variation of the MFS during rolling shows more or less the same behaviour, with two remarks: the MFS values are higher in the case of rolling in comparison with compression during the same temperature conditions for both alloys, however, and the drop for AA6082 was not so drastic as in hot compression. The activation energy values found in axisymmetric compression compare well with those reported

by McQueen et al. [8], with the highest values observed for AA6082. In rolling, the effect of higher values of the MFS was reflected in the values of the activation energies.

Table 2: The calculated values of the MFS and the Activation Energies

AlMg4.5Mn	T°C	MFS (MPa)	Q_{Hw} (kJ/mol)
Compression	RT	315	-
	300	188	170
	400	135	153
Rolling	RT	296	-
	300	235	207
	400	181	193

AlMgSi1	T°C	MFS (MPa)	Q_{Hw} (kJ/mol)
Compression	RT	376	-
	300	119	231
	400	67	168
Rolling	RT	350	-
	300	192	369
	400	125	291

Variation of the flow stresses at the different conditions of temperature, strain and strain rate, are controlled by the chemical compositions and by the mechanisms involved in plastic deformation. The main mechanism for improving the strength of the heat treatable AA6082 alloy is precipitation of a second phase (Mg_2Si) that hinders the dislocation motion at RT; at high temperature, precipitate dissolution takes place, as well as an increase in dislocation annihilation and, subsequently, the rate of softening [9], which will explain the drastic decrease in strength of the metal that was deformed at high temperature. During hot rolling, the material brought from the furnace gets in contact with cold rolls, and this may produce a local surface quench, which may promote dynamic precipitation that leads to strain hardening.

Strengthening of AA5083 is due mainly to solid solution hardening mechanism which depends on the concentration of dissolved atoms that can retard dynamic recovery [10]. In spite the lower values of the MFS at 300 and 400°C, the values of the activation energy of AA6082 were the highest, which may be indicative of the effect of the chemical composition on controlling the activation energy in hot working.

Texture analysis

Fig.3 shows the φ_2 = 0° sections of the ODF of AA5083 measured as a function of processing steps. The texture possesses a cube ({100}<001>) component with an intensity of x8 random, which is often considered as a characteristic of the recrystallized FCC metals with medium to high stacking fault energy [11], and a Brass ({110}<112>) component with an intensity of x7.5. After rolling at 300°C, the Brass component vanishes and the cube texture appears with an intensity of x47 (fig. 3b). Further increase of the rolling temperature to 400°C, destabilizes the {100}<001> orientation (x37), and additional Copper ({112}<111>) and {111}<110> orientations with intensities around x8 appear.

The compression of AA5083 at 300°C gives rise to rotated cube ({001}<110>) with a maximum intensity of x12.5 (fig.4a). Raising the compression temperature to 400°C reduces the cube component to an intensity of about x4, and gives rise to the Brass component with an intensity of x5, and a P-{110}<122> orientation with an intensity of x7.8 (fig. 4b).

The texture of the as received commercial wrought AA6082 is characterized by the presence of a rotated cube-{001}<320> with an intensity of ×13 deviated 10° from the ideal cube position, and a {011}<111> texture component with an intensity of x6, deviated 10° from the position of the ideal P texture component (Fig. 5a). After rolling at 300°C, the cube {100}<001> orientation dominates with an intensity of x22 (fig.5b). Increasing the rolling temperature to 400°C destabilizes the cube component and allows the appearance of a deviated copper ({227}<110>) component and a P-{110}<554> orientation with intensities of x6 and x4.5 respectively.

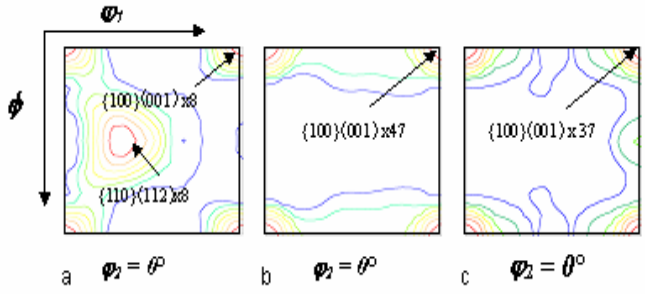

Figure 3: ODF in φ 2 = 0° of Euler space of AA5083 ; a)as received, b) hot rolled at 300°C, c) hot rolled at 400°C.

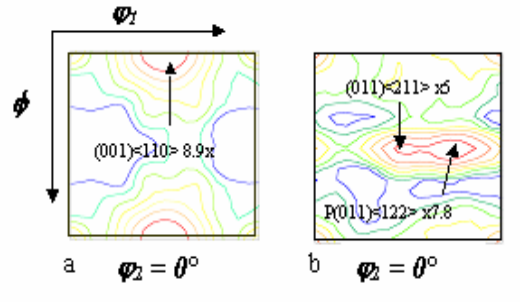

Figure 4: ODF in φ 2 = 0° of Euler space of AA5083 compressed at; a) 300°C, b) 400°C

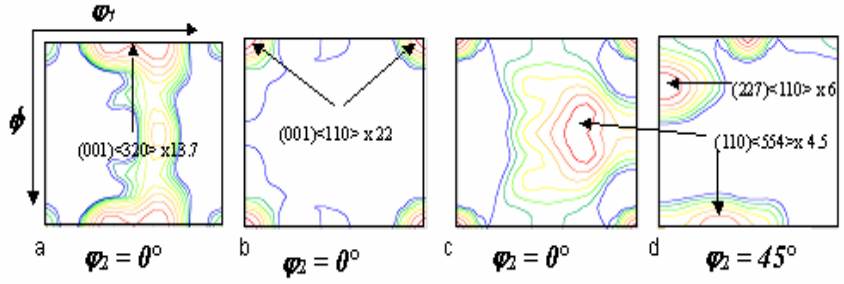

Figure 5: ODF in φ 2 = 0° and φ 2 =45° of Euler space of AA6082 ; a) as received, b) hot rolled at 300°C, c) &d) hot rolled at 400°C

After uniaxial compression at 300°C, the texture consists of a strong cube orientation with intensity around x98, and a weak brass component with intensity of about x12 (Fig. 6a). Increasing the compression temperature to 400°C, causes cube component to fall by a factor of 10.

It is well known that preferred orientation is developed during the rolling of aluminium alloys [11]. The influence of the deformation technique and the working temperature on the texture of both alloys is reflected by the results of the OIM analysis. This difference in the developed texture is due mainly to the mechanisms controlling each deformation mode, and the recrystallization processes in both alloys. In AlMg4.5Mn alloy, the higher content of Mg inhibits dynamic recovery by restricting dislocations mobility and inhibiting the grain boundary migration, which enhance the recrystallization process during hot rolling [12].

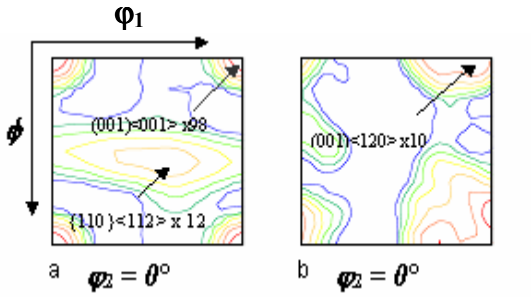

Figure 6: ODF m easurement (φ 2 = 0°) of compressed AA5083; a) at 300°C, b) at 400°C

On the other hand, limiting the migration of the grain boundary reduce the preferred growth of the cube oriented grains [13]. However, the presence of a strong cube texture in AA5083 after hot rolling than after hot uniaxial compression is due mainly to the fact that flat rolling is essentially a plane strain operation, and as consequence the strain and stress distribution will be different than in axisymmetric compression, which can have an influence on the solutes concentration near the grain boundaries and their action to limit boundaries migration.

For AlMgSi1, the contribution of particle-simulated nucleation (PSN) to recrystallization is very important. It seems that the nuclei originate in the deformation zone and their orientations are restricted to those present in these zones [11]. Habiby and Humphreys [14] have shown that even if PSN grains are highly misoriented from the matrix grains, a weakened rolling texture would results. The weak texture of AA6082 after rolling at 300°C can be attributed to the nucleation in the deformed zones around the second phase. In the other hand, the strong cube texture present after compression at 300°C can be a sign of the nucleation of Cube oriented grains on transition bands [13].

CONCLUSION

The values of the mean flow stresses and the activation energies obtained after the laboratory flat rolling and the axisymmetric compression are comparable to each other for AA5083 and AA6082 alloys. However the textures developed are quite distinct. This is due mainly to difference in the mechanisms controlling the plastic deformation and the recrystallization in each deformation technique for the tested alloys.
Axisymmetric compression can be an appreciable technique to give information about some mechanical and physical parameters needed to simulate flat rolling, but not favorable enough to simulate the developed texture.

REFERENCES

1. E. Voce, J. Inst. Met. 74 (1948) pp 537.
2. A. Airod, H.V. Kinderen, J. Baros, R. Colas, Y. Houbaert, J. Mat. Proc. Tech. 134 (2003) 398-404.
3. R. B. Sims; Proc. Ins. Mech. Engrs, 168 (1954), 19.
4. T. M. Maccagno, J. J. Jonas, S. Yue, B. J. McCrady, R. Slobodian and D. Deeks; ISIJ Inter. Vol. 34 (1994), No. 11, pp. 917-922.
5. C.M. Sellars and W.J. McG. Tegart: Int. Metall. Rev., 1972, vol. 17, pp. 1-24.
6. J.J. Jonas, C.M. Sellars and W.J. McG. Tegart : Int. Metall. Rev., 1969, vol. 14, pp. 1- 24.
7. A. Airod, R. Colàs and Y. Houbaert; Plastic Deformation of 1050, 5083 and 6082 Aluminium Alloys". COM 2003, Vancouver, Canada.
8. H.G. McQueen, N.D. Ryan; Mater. Sci. Eng. A322 (2002) 43-63.
9. W.Shyan Lee, W.C. Sue, C.F. Lin, C.J. Wu, J. Mat. Proc. Technol. 100 (2000), pp 116-122.
10. C.A.P. Horton, Acta Metall., 20 (1972), pp 477.
11. F.J. Humphreys and M. Hatherl, "Recrystallization and Related Annealing Phenomena", Great Britain, Pergamon, 1995).
12. M.A. Wells and D.J. Lloyd; Hot Deformation of Aluminum Alloys II, The Minerals, Metals & Materials Society, 1998.
13. K. Lùke and O. Engler; " Recrystallization Texture in Heat Treatable and non Heat treatable Aluminium Alloys", ICAA3, P. 439-452.
14. F. Habiby and F. J. Humphreys (1993), Text. Microstruct. 20, 125.